JOURNAL OF GEOPHYSICAL RESEARCH, VOL. 101, NO. B3, PAGES 6099–6108, MARCH 10, 1996

Holocene slip rate of the Hayward fault at Union City, California

James J. Lienkaemper
U.S. Geological Survey, Menlo Park, California

Glenn Borchardt
Soil Tectonics, Berkeley, California

Abstract. Measured offsets of well-dated alluvial fan deposits near the Masonic Home in Union City constrain Holocene slip rate of the Hayward fault between 7 and 9 mm/yr. Our best minimum geologic slip rate over the past 8.27 ± 0.08 kyr (i.e., 8270 years) is 8.0 ± 0.7 mm/yr. A steep stream (its channel cut into bedrock) flows southwest out of the East Bay Hills, crosses the fault, and deposits its load on an alluvial fan. We cut two 5-m-deep, fault-parallel trenches 20–30 m southwest of the main fault through the crest of the fan. Walls of the trenches reveal a series of nested distributary channel fills. These channels had cut into old surfaces that are indicated by paleosols developed on flood silts. We distinguished many channel fills by their shape, clast size, flow direction, elevation, and relation to paleosols, enabling us to correlate them between both trenches. Two distinct episodes of fan deposition occurred during the Holocene. Reconstructing the apex positions of these fan units indicates that about 42 ± 6 m and 66 ± 6 m of fault slip has occurred since their inceptions at about 4.58 ± 0.05 ka, and 8.27 ± 0.05 ka, respectively. We lowered the age and age uncertainty of the younger unit from earlier reports based on new multiple radiocarbon dates. The 4.58 ka slip rate of 9.2 ± 1.3 mm/yr is not significantly different at 95% confidence from the 8.27 ka slip rate of 8.0 ± 0.7 mm/yr. Because current regional strain rates are fully consistent with Neogene plate tectonic rates (Lisowski et al., 1991) and the historic surface rate of creep in Union City is only 4.7 ± 0.1 mm/yr (Galehouse, 1994), the larger, ≥8 mm/yr, Holocene slip rate implies that strain is now accumulating on a locked zone at depth. The 8 mm/yr rate is probably minimal because earlier trenching evidence nearby implies that some unknown additional amount of fault deformation occurs outside of the narrow fault zone assumed in measuring slip. Lienkaemper et al. (1991) suggest that the fast creep rate of 9 mm/yr, measured near the southern end of the Hayward fault, may underestimate the deep slip rate, because 1868 surface slip occurred there in addition to the continuing fast creep. If the historic deep slip rate equals the long-term rate, then the 9 mm/yr creep rate reflects the minimum seismic loading rate of the Hayward fault better than the ≥8 mm/yr Holocene rates do.

Introduction

For the 6 million people in the San Francisco Bay region, the most centrally located fault segments expected to produce major ($M \sim 7$) earthquakes in the next few decades are the northern and southern segments of the Hayward fault. These segments last ruptured in major earthquakes in 1836 (probably) and 1868 (certainly), respectively [*Working Group on California Earthquake Probabilities*, 1990]. The risk currently posed by the Hayward fault is especially high because more vulnerable older structures on soft soils are concentrated near the Hayward fault than near other high-probability fault segments in the region [*Steinbrugge et al.*, 1987; *Perkins*, 1992].

Where detailed long-term recurrence histories are unavailable, estimating earthquake probability and characterizing the source and recurrence process of major earthquakes depends on many variables. However, for simplicity, the three most important variables are the long-term or geologic slip rate of the fault, the coseismic slip in the source region, and the expected length of rupture. The earthquake process of the Hayward fault is especially hard to assess because creep occurs steadily at about 5 mm/yr, releasing a significant fraction of crustal strain near the surface [*Lienkaemper et al.*, 1991]. Detailed discussion of the complex source process and of the resulting earthquake hazard is beyond the scope of this paper, but understanding and constraining this process is the underlying motivation for investigating the long-term slip rate of the Hayward fault.

The Hayward fault is part of the San Andreas system of strike-slip faults (Figure 1) [*Wallace*, 1990]. How the component faults of the system, the San Andreas, Hayward, and Calaveras, interact over the short term (e.g., decades) and long term (e.g., centuries and millenia) is far from certain [*Lisowski et al.*, 1991; *Savage and Lisowski*, 1993; *Brocher et al.*, 1994]. The purpose of this paper is to document the best available long-term or geologic slip rates on the Hayward fault because they have an important bearing on the problems of earthquake probability and fault system mechanics alluded to above.

It is important to be aware that geologic slip rates commonly

Paper number 95JB01378.
0148-0227/96/95JB-01378$05.00

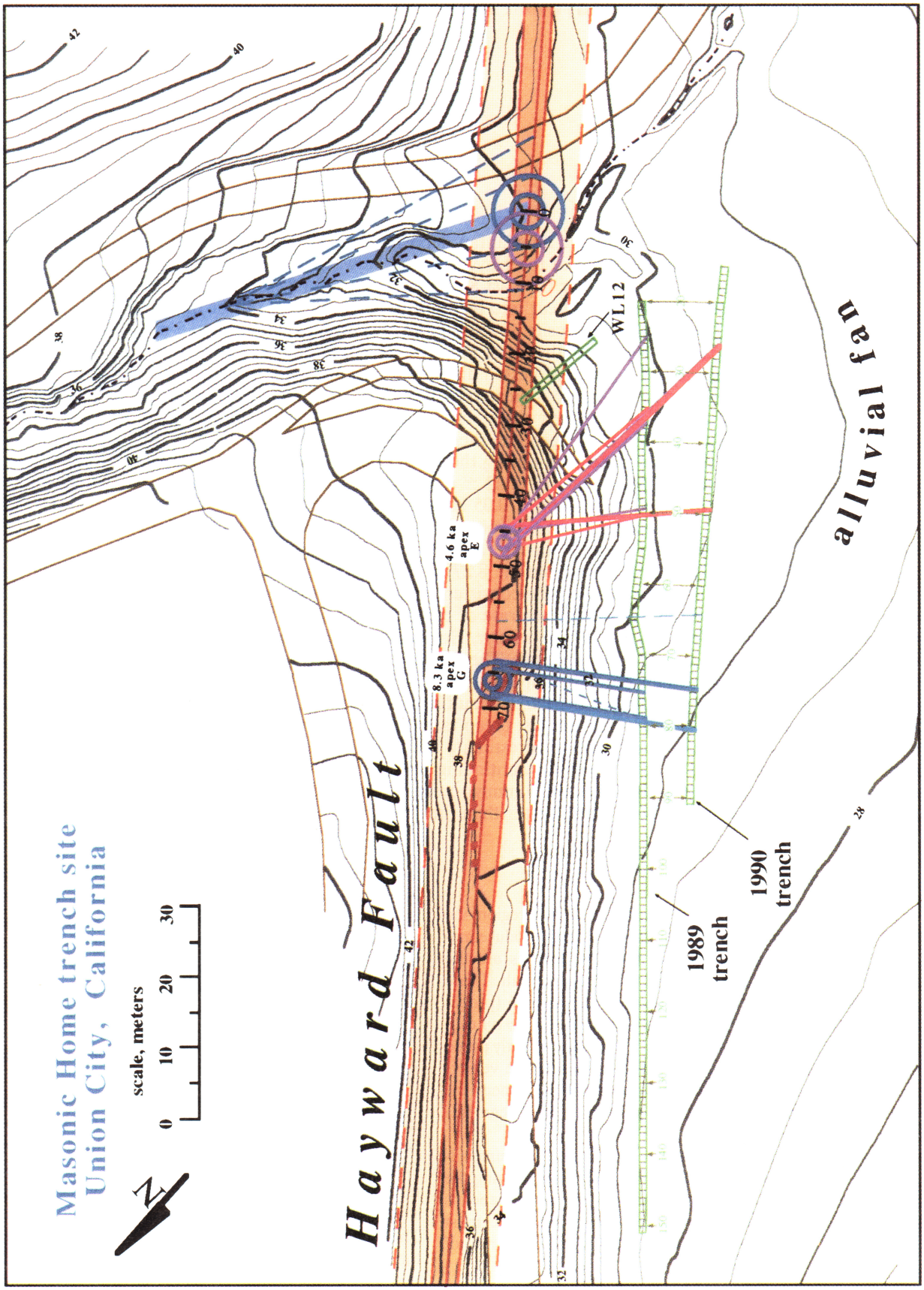
Masonic Home trench site
Union City, California
scale, meters
0 10 20 30
N
Hayward Fault
alluvial fan
1989 trench
1990 trench
WL12
4.6 ka apex E
8.3 ka apex G

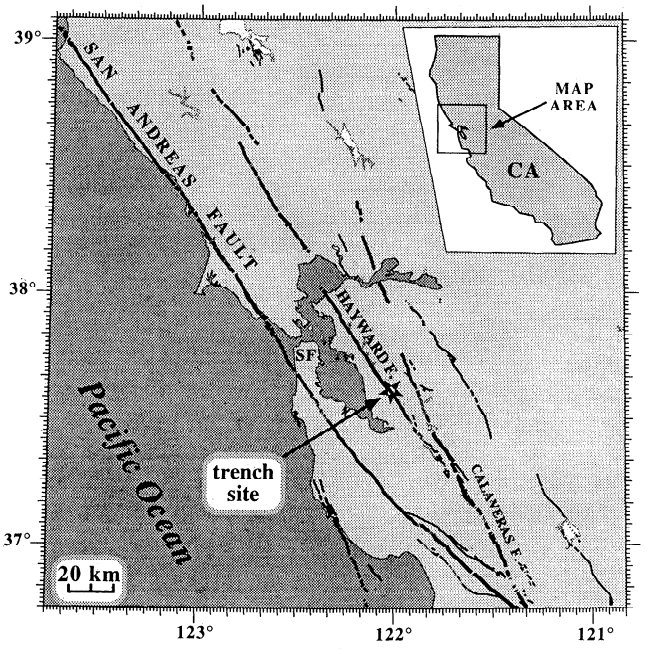

Figure 1. Location of Masonic Home trench site.

suffer from the defect that they tend to underestimate the entire slip rate of a fault zone. The geologic markers used to measure slip, such as stream channels, are often short compared to the full width of the deformation zone; thus they do not allow measurement of the total slip. An earlier effort to measure geologic slip rate on the Hayward fault in Fremont [*Borchardt et al.*, 1992] was seriously flawed by this problem, thus leading to this work on a narrower deformation zone at the Masonic Home site in Union City.

Geologic Setting of the Masonic Home Site

The location of the Masonic Home site is indicated in Figure 1 (for a more detailed map, see km 55.1 of *Lienkaemper* [1992a, b]. Our investigation benefited from extensive earlier trenching work done on this and the adjacent site by consultants (Woodward-Lundgren (unpublished report, 1972) and Burkland and Associates (unpublished report, 1972); for full references and access to these reports, see *Lienkaemper* [1992a].) The earlier trenching revealed evidence of Holocene thrusting and reverse components of slip nearby, ~100 m southeast of our site, that extend ≥20 m southwestward of the main fault trace. Thus the entire area of our trenching investigation is likely to be within a zone of some distributed deformation, and this factor must be considered in our conclusions about completeness of slip rate. The pre-Quaternary geology of the site and drainage area [*Dibblee*, 1980] does not enter strongly into the solution of the Holocene slip rate problem. However, the Orinda Formation, composed of Pliocene continental deposits, does provide an unusual abundance of clay to the fan and is the dominant source of a wide variety of reworked clasts in the Holocene deposits. The Monterey Formation, a Miocene marine shale and chert unit, contributes abundant but mostly angular clasts because it crops out only 0.5–0.7 km upstream.

The focus of our slip rate problem involves documenting the progressive offset of the apex of alluvial fan deposits from the

Plate 1. Site map. Contours in 0.5-m intervals based on topographic map prepared using total station instrument (distances and angles measured electronically). Main trace of fault shown as solid red lines (e.g., en echelon shears in driveway) and dark reddish pattern; lighter reddish pattern indicates zone of secondary deformation and meanders in main trace; numbers indicate offset (in meters) of apex G from canyon mouth. Northeast of fault, shaded blue line is interpreted 8.27 ka canyon centerline; adjacent blue bullseye is zero point for apex G offset; adjacent purple bullseye is interpreted zero point of apex E (accounts for downcutting). Southwest of fault, offset apex positions G and E defined by piercing points of gravel-filled channels projected to fault (unit colors defined in Plate 2); thick lines are based on southwest walls of 1989 and 1990 channels; narrow lines from projecting channels from both walls of 1989 trench. WL12, trench by Woodward-Lundgren (unpublished report, 1972) (see *Lienkaemper* [1992a] for full reference). Brown lines are roads.

mouth of a perennial stream channel (~0.75 km^2 drainage area) that emerges from the hills northeast of the fault (Plate 1). Our initial trenching effort in 1989 revealed that a cyclic geomorphic process of fan-apex abandonment has occurred at least 6 times at this site over at least the last 20,000 years [*Lienkaemper*, 1990]. As right-lateral slip accumulates, by a combination of interseismic creep and coseismic slip during major earthquakes, the established fan apex moves northwestward along the fault. The apex continues to be fed by a newly-formed segment of channel that runs alongside the fault. It is important for the reader to understand that coseismic slip in large Hayward fault earthquakes is relatively small, about a meter or less [*Lawson*, 1908; *Lienkaemper et al.*, 1991; *Lienkaemper and Hamilton*, 1992]. Thus we are not documenting the amount of slip occurring in any one earthquake but rather the slip that has accumulated from several earthquakes and millenia of creep. Our trenching evidence showed that because the channel is flowing along the fault and at the apex is naturally entrenched by a few meters (1–3 m), as much as 20–50 m of slip can occur before a new fan apex forms [*Lienkaemper*, 1990]. As the offset increases, the gradient of the channel segment parallel to the fault becomes lower and lower. Eventually, the channel gradient becomes too low for the stream flow to transport its bed load. The channel fills initially with coarse-grained deposits and finally reaches a ponding stage in which the channel is sufficiently filled so that substantial storm flows can overtop the channel wall barrier. A new channel is cut approximately straight outward from the canyon, crossing the fault to form a new apex.

Stratigraphy of the Site

Strategy and Methods

The strategy for trenching this fan was limited by two practical constraints. First, the length of the initial trench in 1989, ~130 m, was chosen as being entirely within reach of radiocarbon dating for a presumed range of possible slip rates. Second, we had to maintain a distance of 3 m from the primary sewer line of the Masonic Home. Trenching nearer the fault, upslope from the sewer, was inhibited by steep slopes, large trees and a 3- to 5-m-thick fill underlying the principal access road to the Masonic Home. The long 1989 trench was logged quickly (1.5 months) compared to the shorter (~75 m) 1990 trench (2.5 months) because of financial and land use constraints and was thus more of a reconnaissance effort. Nevertheless, the most important elements of the stratigraphic sequence were distinctly recognizable in both the 1989 and 1990 trench logs (Plate 2). We found clear evidence for six packages of fan sediments stacked younging southeastward along the fault. Each package of fan deposits is associated with a distinct apex position as discussed above (see *Lienkaemper* [1990] for locations of Pleistocene apexes). We have referred to these sedimentary packages as apex units: M (not on Plate 1), K, I, G, E, and C. Plate 2 shows further division of apex G and E deposits in subunits G1, G2, E0, E1, and E2. The usage of terms CU, IU, and KU in Plate 2 only indicates that these units are undifferentiated into subunits for purpose of this report. The expression "deposits of apex unit I" has the same meaning as "apex unit IU"; "apex unit G" also means the same as "apex unit G undifferentiated"; and so forth. The strategy in 1990 was to focus on verifying the accuracy of piercing points for apexes G and E. This paper focuses almost entirely on apex units G and E in order to document their respective ages and amounts of fault slip.

Plate 2 is a 6 times reduction and simplification of the southwest walls only of field logs that were drawn for both walls of each trench on transparent mylar sheets. The use of transparent logs allowed easily detailed comparison of channel morphology and exact determination of flow directions by flipping over and overlaying logs of opposite walls on a light table. We scanned all the field logs for drafting digitally and have archived these scans and drafting on optical media. Copies of this field archive can be obtained for the cost of reproduction by arrangement with the authors. The meter grid shown on Plate 2 was laid out using a steel tape and a water level. We refer to the longitudinal direction as "x" or "station" and the vertical as "z" or "elevation." We established control of the map coordinates and the site datum using permanent bench marks and an electronic surveying instrument. The actual location of the trench x coordinate grid is shown in Plate 1. The elevations on the map are approximately the elevation above sea level. The arbitrary datum for the trench grid has the value of 6.515 m at the map elevation of 30 m. For example, the stream now flows across the fault at ~6.8 m relative to the trench grid datum or ~30.3 m in elevation above sea level.

Pleistocene Apex Unit I as Prelude to the Holocene Apex Units

Although we recognized three late Pleistocene apex units in the northern part of the 1989 trench, we will discuss only those aspects of the deposits of the youngest Pleistocene apex (unit I) as they relate to the transition to the early Holocene apex unit G (see *Lienkaemper* [1990] for map and further discussion of Pleistocene units). We will not discuss the other Pleistocene apexes herein because of two major problems. First, the Pleistocene channels are generally much broader and appear to meander much more than their Holocene counterparts, rendering them less suitable for measuring slip. An exception to this is the terminal stages of unit I (~9 ka) when the more modern narrower channel form had begun. Second, the age control on these units is distinctly poorer than for units of the Holocene, as we found much less charcoal in them. As we discuss below, it is important to bracket the basal age of each unit as closely as possible and with enough redundancy to guard against stratigraphically false ages, which we recognized in about one in every four Holocene samples.

Probably the most important aspect of the Pleistocene story at the site is that it helps constrain our recognition of the onset of apex unit G deposition, the first purely Holocene episode of fan building. From our trenches southwest of the fault, we know that apex unit I began as broad channels and apparently was associated with a 45- to 50-m-wide abandoned terrace located 70–130 m northeast of the fault (not shown in Plate 1; shown by *Lienkaemper* [1992b]) that narrows to about 30–40 m wide nearer the fault. This terrace was abandoned by the onset of incision within 70 m of the fault probably beginning between 13 ka and 10 ka, when the channel shape became narrower. One of the underlying causes of this incision must involve tectonic uplift. The terrace is remarkably smooth and projects 5.1 ± 0.1 m above the modern stream at the fault. This vertical separation suggests a minimum vertical slip rate of 0.4 mm/yr. However, to obtain the true vertical slip rate, we must match the terrace to the present elevation of buried apex unit I as preserved in trench logs. The top of unit I implies at least 0.5 mm/yr, and its base suggests at most 0.7 mm/yr of vertical slip

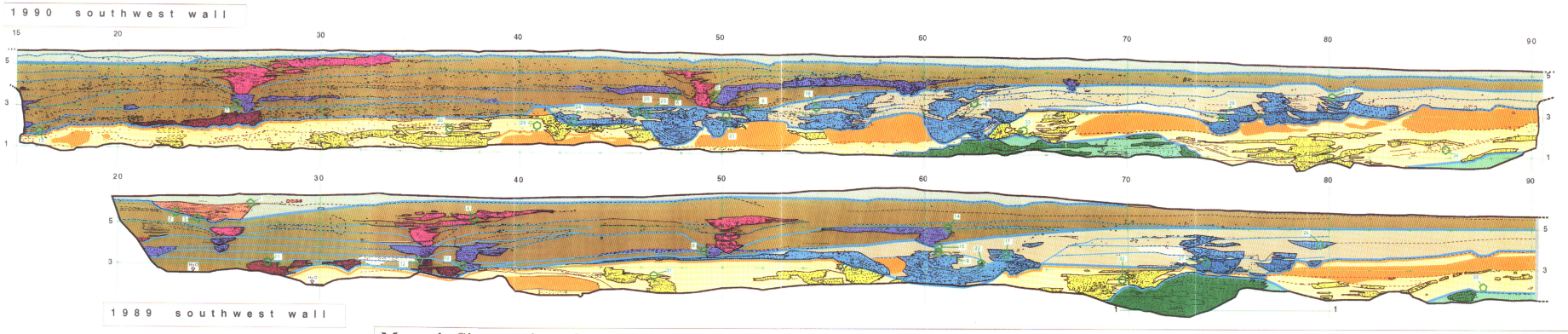

Masonic Site stratigraphy

Channel Fills

	fan apex unit	probable basal age, yr	range of ^{14}C dates (in stratigraphic order)†
CU	undifferentiated	600	490 580 630
E2	upper	4100	2840 4100
E1	lower	4580	4730 [6080]§ 4250 4730 4640
E0	basal	4580	[6220]§ [3020]§ 4560
G2	upper	7230	[5580]§ [6620]§ 4980 5050 5100 5940 [6720]§ 5210 5100 7060 [7080]§ [5910]§ 7390
G1	basal	8270	8270 8270
IU	undifferentiated	~13,520	[8780]§ 10,240 8510 12,970 8900 8920 13,520

Channel Fills and Flood Deposits

KU	undifferentiated	~17,170	17,170 sample from station 121 m of 1988 bench

Soils

CO_3 soil	upper	Age range with weaker carbonate development	7230 8270
CO_3 soil	lower	Age range with strong carbonate development	8270 10,240

Flood Deposits

CUF	undifferentiated	600	see associated channel fill ages
EUF	undifferentiated	4580	ditto
GUF	undifferentiated	8270	ditto
IUF	undifferentiated	~13,520	ditto

† calibrated ages before 1990, see Table 1

[8780]§ - carbon date judged older than deposition date, see Table 1

[8780]§ - carbon date judged younger than deposition date, see Table 1

Symbol key

- Carbon-14 sample location
- Carbon-14 sample location (opposite wall, equivalent horizon)
- clast, actual size & location
- gravel (<5 cm) generalized
- k krotovina (filled burrow)

Grid is in meters

Plate 2. Trench logs.

rate. Because the terrace was probably abandoned between these two stages, 0.6 ± 0.1 mm/yr is probably a reasonable estimate of Holocene vertical slip rate for the site, although it would be interesting to test this hypothesis by dating this terrace. A smaller surface offset of ~1.3 m on sediments aged ≤2.8 ka, shown in the log of a 1972 trench of Woodward-Lundgren (WL12, Plate 1), suggests a vertical slip rate of ≥0.5 mm/yr.

Another less certain factor relating to incision is climate. At about 10 ka, carbonates began to precipitate within the flood silts at the fan surface. By the onset of deposition from apex G at 8.27 ka, well-developed carbonate soils had formed. Carbonate formation is usually associated with arid and semiarid environments. The channel style change and thus the deep incision northeast of the fault occurred between 13 and 10 ka before evidence of soil carbonate formation. Consequently, we can reasonably state that the early period was wetter and possibly that the greater rainfall caused the abandonment and incision. Alternatively, because fault uplift created an erosionally unstable environment for the terrace, incision may have begun simply as a temporally random process.

The terminal phase of apex I is dated about 8.5 ka (e.g., charcoal sample 30, Plate 2 and Table 1). These last deposits from apex I contain among the largest boulder clasts, similar to the latest deposits from the G apex. This increase in clast size is surprising as the stream gradient diminishes with offset, and so does its power to flush the boulders farther downslope. Another characteristic that these later stage channel deposits share is their low angle to the trench wall. Later stage deposits are usually forced southward away from the high crest of the mature fan and rarely deposit to the northward because of the lopsided sedimentation imposed by strike-slip abandonment of the older fan deposits. We deduce that the surprising increase in clast size in the later stages of deposition from apexes I and G is the effect of temporary rejuvenation. When the new southwestward flow begins, the gradient is steep again, and very coarse materials are flushed from the fault-parallel segment. Soon, however, the process ends as the gradient again becomes lower than ever, and tectonic abandonment is completed.

Holocene Apex Units G, E, and C

The basal subunit G1 of apex unit G cuts into the well-developed carbonate soil of apex unit I. These subunit G1 gravels are located distinctly southwestward of the crest of the apex I fan and flowed with high energy directly outward from the canyon mouth; thus they represent a straightening of the stream across the fault. We measured the flow directions using exact matches of channel centers and margins of two channels on opposite walls of the 1989 trench. Projecting these channels to the fault gives 64–68 m of right-lateral slip, as shown by the thinner blue lines in Plate 1. We use the canyon centerline northeast of the fault shown in Plate 1 as a reasonable reconstruction of the canyon centerline at 8.27 ka, which we will discuss further below. A burn layer, or deposit of abundant charcoal chunks, in the top of the stratigraphically lowest gravel in unit G was sampled in both 1989 and 1990 trenches (samples 27 and 28), which resulted in identical tree ring calibrated radiocarbon ages of 8.27 ka for both trenches.

The piercing points derived from matching the two most distinctive gravelly channel fills in both trenches (using logs of the southwest walls) gave a range of 63–69 m slip. These data provide a check for the location of basal apex unit G at the fault. The mean of these four piercing-point determinations is 66.0 ± 2.5 m (single-standard deviation error for southwest side only). It is important to understand that this error only represents the piercing-point uncertainty. The total error in estimating slip is heavily dominated by uncertainty in estimating the position of the canyon center as it has changed through time, which we discuss in the next section.

The active channels from apex G remained near the crest of the fan until after 7.2 ka (samples 25 and 26), but before 6 ka (sample 24), they diverted southward (at a very low angle to our trench walls) and incised through the flood silts from apex G1 and cut more than 1 m into the carbonate soils developed on apex unit I. An unusual pedestal of carbonate soil at $x = 58$ m shows how a bouldery channel of subunit G2 with a flow direction virtually parallel to the 1989 trench line incised a vertical wall into the carbonate soil of apex unit I age. The low angles of the youngest subunit G2 channels rule out any reasonable likelihood that they emanate from apex E, which is distinctly located by later units. Some possibility remains that after 7.2 ka, another apex, F(?), could have formed, but we view this as unlikely and it is only permissible because the deposits in latest subunit G2 time are among the most erratic and hard to match, even across a single trench. We can only say that these gravels flowed from a source distinctly nearer to apex G than to apex E. Fortunately, the existence of apex F(?) is irrelevant to solving for slip rate for the highly distinct apexes G and E.

Apex E was identified clearly in 1989, principally based on three sets of nested channel fills near stations 25, 35, and 50 m. The amount of slip for apex E was already well-constrained because the flow directions as measured from both walls of the trenches on many channels project to the fault in a tight cluster. For example, the five clearest matches (shown as narrow lines in Plate 1) have a mean value of slip of 46.3 ± 0.6 m (less 5 m as discussed below). Using the 1990 log along with the 1989 log, the three clearest matches, shown as wider lines in Plate 1, yield a mean slip of 46.8 ± 2.2 (also less 5 m as we discuss below) suggesting that channels become more sinuous as they become distal. For slip rate calculation we combine all of the eight clearest piercing points in apex unit E for a mean slip of 46.5 ± 0.6 m. From this we subtract 4.9 m, which accounts for the proportionate northward drift of the canyon center between its position at 8.27 ka and the present position of the stream bottom. Thus we reckon slip to be 41.6 m. We explain this analysis further in next section. Again, as in the preceding discussion for apex G, the above uncertainties in slip reflect only the single standard deviation errors from the piercing-point analysis alone. The total error estimate of slip is strongly dominated by uncertainties in the canyon center as we discuss in the next section.

The age of apex E was problematic in 1989 because we obtained three radiocarbon dates (samples 7, 11, and 14) that violated the stratigraphic sequence in the lowest part of apex unit E and near the contact with apex unit G. Our more detailed work in 1990 to refine the stratigraphy of basal strata in apex unit E and the terminal strata in apex unit G included intensified sampling of charcoal. We collected over 500 samples during the entire investigation. A high density of similar radiocarbon dates in basal apex subunits E0 and E1 (samples 6, 8, 9, 10, and 13) yields a mean value of 4580 ± 50 years for the calibrated age of apex E. Although the samples are clearly from slightly different stratigraphic horizons, the size of the individual laboratory errors renders these differences statistically insignificant. Further attempts to refine the age and re-

Table 1. Radiocarbon Dates on Charcoal

Sample			Year and Wall	Location on Log		Fan Apex Unit	Age	
Sed. Seq.	Field	Lab		*x*, m	*z*, m		Radiocarbon years B.P.	Calibrated,* years pre-1990
1	89B341	AA-4657	89E	26.7	6.1	CU	415 ± 60	490 ± 70
2	89B134	I-15,819	89W	28.9	5.5	CU	510 ± 80	580 ± 70
3	89B142	AA-6814	89E	24.6	5.4	CU	580 ± 70	630 ± 40
4	89B162	AA-8906	89W	37.6	5.3	E2	2665 ± 60	2840 ± 60
5	90B161	AA-4649	90W	49.7	3.8	E2	3700 ± 60	4100 ± 90
6	90B158	AA-6816	90W	47.7	3.9	E1	4150 + 60	4730 + 90
7	90B283	AA-6813	90W	25.8	3.2	E1	5240 ± 60	[6080]† ⊥ 80
8	89B271	AA-4653	89W	49.1	3.8	E1	3800 ± 100	4250 ± 140
9	90B166	AA-6817	90W	51.3	3.2	E1	4160 ± 60	4730 ± 90
10	89B175	AA-4651	89W	37.1	3.0	E1	4065 ± 100	4640 ± 140
11	89B139	AA-4648	89E	29.1	3.2	E0	5400 ± 100	[6220]† ± 120
12	89B201	AA-8907	89E	35.3	3.3	E0	2845 ± 50	{3020}† ± 80
13	90B314	AA-6824	90W	16.2	1.7	E0	4000 ± 70	4560 ± 130
14	89B292	AA-4654	89E	60.8	5.1	G2	4805 ± 60	[5580]† ± 80
15	89B300	AA-8909	89E	60.4	4.3	G2	4395 ± 60	5050 ± 110
16	90B193	AA-11,598	90W	54.7	3.2	G2	5845 ± 70	[6720]† ± 90
17	89B274	AA-8908	89E	65.3	3.8	G2	4520 ± 50	5210 ± 80
18	90B212	AA-9603	90W	62.5	3.5	G2	6145 ± 70	[7080]† ± 80
19	89B298	AA-4655	89E	61.0	3.8	G2	5750 ± 100	[6620]† ± 110
20	90B142	AA-6822	90W	45.7	3.0	G2	4430 ± 60	5100 ± 120
21	90B162	AA-11,597	90W	50.2	2.8	G2	4420 ± 80	5100 ± 130
22	89B312	AA-8910	89E	63.5	3.5	G2	5135 ⊥ 60	[5910]† ± 70
23	90B144	AA-8912	90W	46.3	2.9	G2	4320 ± 50	4950 ± 60
24	90B108	AA-8911	90W	42.6	2.6	G2	5145 ± 70	5940 ± 90
25	90B262	AA-6820	90W	80.2	3.9	G2	6110 ± 60	7060 ± 90
26	89L013	AA-4660	89W	79.6	4.2	G2	6470 ± 120	7390 ± 100
27	89B031	AA-4259	89W	74.0	3.3	G1	7435 ± 60	8270 ± 80
28	90B222	AA-6815	90W	74.7	2.8	G1	7430 ± 70	8270 ± 90
29	90B105	AA-6823	90W	40.9	1.3	IU	7890 ± 100	[8780]† ± 150
30	90B090	AA-6818	90W	36.4	2.1	IU	7680 ± 70	8510 ± 80
31	89B191	AA-4652	89W	46.6	2.5	IU	7740 ± 110	8600 ± 160
32	89B349	AA-4658	89W	69.7	2.5	IU	8055 ± 130	8920 ± 160
33	90B214	AA-6819	90W	64.9	2.2	IU	9260 ± 70	10,240 ± 5
34	90B249	AA-6821	90W	85.5	1.5	IU	11,010 ± 80	12,970 ± 90
35	89L033	AA-4663	89E	87.0	2.4	IU	11,560 ± 100	13,520 ± 140

Sed. seq., sample numbers follow inverse of sedimentation sequence (Plate 2). Lab is NSF-Arizona AMS Facility, University of Arizona, Tucson, except 89B134, which is Teledyne Isotopes, Inc., Westwood, New Jersey.

†Stratigraphically inconsistent date indicates reworked charcoal or laboratory mistake: brackets indicate old date, reworked from older alluvial units or burning of old wood and braces indicate young date, reworked from surface by soil or biological process.

*Using program CalibETH 1.5b (ETH Zürich, 1991) and ATM20.C14B calibration file [*Linick et al.*, 1986]. Sample 90B214 was calibrated using file Stuiver3.C14B [*Stuiver*, 1991]. Samples 90B249 and 89L033 corrected using calibration program of *Stuiver and Reimer* [1993], revision 3.0.3c.

duce its error, such as using the methodology of *Biasi and Weldon* [1994], would not significantly improve the age estimate for apex E. Thus we conclude that the age of inception of flow from apex E to be 4.58 ± 0.05 ka.

Flow was still directed out of apex E until 2.8 ka (sample 4), but by 0.6 ka (samples 1, 2, and 3), flow was from a new apex (C). This change was evidenced by only one gravel channel fill in the 1989 trench at $x \sim 25$ m with a flow direction that indicates slip of roughly 5–15 m. We made no further attempt to constrain the apex C slip rate because it would require extensive work in the saturated stream environment with little hope of obtaining a slip rate as accurate as the other Holocene rates.

Analysis and Discussion of Uncertainties in Slip

The principal source of uncertainty in measuring slip and hence slip rate is from geomorphic interpretation of the stream channel centerline in the canyon northeast of the fault. Other evidence pertinent to the interpretation is related to the downcutting of the channel as it was described above in the section on the Pleistocene apex unit I. Our interpretation is illustrated in Plate 1. A large shaded blue line in the canyon shows our interpreted best fit of the early Holocene centerline. This interpretation rests on the following assumptions: (1) incision into the late Pleistocene terrace from 13 to 10 ka created the overall shape of the 55-m-long reach of the stream just above the fault; (2) a vertical slip rate of 0.6 mm/yr would place the 8.27 ka location of the stream channel center at elevation 32 m (5 m uplift less the 3 m of ponded deposits from the terminal phase of apex E age which probably covers the modern canyon bottom); and (3) erosion of the canyon mouth with its present right-lateral kink is dominantly a post-8.27 ka phenomenon related to downcutting and natural backfilling caused by the tectonic obstruction. A blue bullseye at the fault is our best estimate of the position of apex G at 8.27 ka. An inner set of dashed blue lines in the canyon represents the extrapolation of the channel bottom from the less eroded area above the fault.

This interpretation gives the most reasonable position and a likely range of ±5.5 m of slip. We believe this value is comparable to single standard deviation error. Our outer blue dashed lines at ±11 m are what we consider physically possible limits of error. If this could be translated to statistical confidence, we believe it would be roughly comparable to two to three standard deviations.

Similarly, the purple bullseye indicates our interpretation of the likely range of ±5.5 m of error in slip inferred from apex E deposits. The position is determined analytically by assuming that the downcutting and the northward shift of the channel at the fault has proceeded as a steady process from 8.27 ka until present. Thus the fraction (8.27 − 4.58) ÷ 8.27 is the proportion of the 11-m distance between the apex G position at 8.27 ka and the present channel center (i.e., 4.9 m) that gives the shift occurring from 8.27 to 4.58 ka. Plausible arguments can be made for placing the 4.58 ka channel at either endpoint of this 11-m range. However, we favor using this analytical position because it can be argued as more probable than the two extreme positions, but using the full range is not compatible with a Gaussian distribution. For example, the error, ±5.5 m, can be used cautiously as similar to a single standard deviation. However, if one doubled this "single standard deviation error," then the error is constrained unevenly (e.g., −11 m is barely plausible, but +11 m is not plausible given the reasonable constraint of generally steady erosion; the channel was forced northward as it cut downward over time).

A problem that frequently hampers determining strike slip on buried channels is that the possibility of some initial amount of apparent strike slip can never be entirely ruled out. However, we believe this site is among the most suitable for avoiding and minimizing this possibility because the fault zone is relatively narrow and for the reasons that follow. Most importantly, the existence of a sizeable vertical component, ~0.5 or 0.6 mm/yr, helps maintain a high stream gradient and thus high flow velocity across the fault, which strongly favors the establishment of straight channels. The coarseness of the gravelly deposits attests to this high flow velocity. Also important is recognition of distinct basal units that demonstrate the reinvigorated flow regime. We believe that serious sinuosity problems are reasonably likely only within the canyon mouth environment (and terminal phase fan apex deposits) and are reasonably well-incorporated into the error ranges discussed above. Furthermore, our emphasis on the 8.27 ka slip rate as being the best overall measurement reflects the robustness of having averaged a large amount of slip and thus making less important many of the uncertainties of initial channel configuration that affect the determinations of smaller stream offsets.

Calculation of Slip Rate and Its Uncertainty

For apex G, slip ($\mathbf{d_G}$) is ~66 m, and it has single-standard-deviation uncertainty in the slip (ε_d) of ~6 m, that is calculated as a root-mean-square error (ε_{rms}) sum of the southwest-side error ($\varepsilon_{\mathbf{SW}} \sim 2.5$ m) and the northeast-side error ($\varepsilon_{\mathbf{NE}} \sim 5.5$ m). For example, $\varepsilon_{\text{rms}} = \{\varepsilon_{\mathbf{SW}}^2 + \varepsilon_{\mathbf{NE}}^2\}^{1/2}$, where $\varepsilon_{\mathbf{SW}}$ and $\varepsilon_{\mathbf{NE}}$ are errors associated with estimating the stream channel intercepts with the fault from each side of the fault. Age ($\mathbf{t_G}$) of inception of flow from apex G is 8270 years (before 1990) and single-standard-deviation uncertainty in the age (ε_t) is 80 years. We thus calculate a slip rate ($\mathbf{d_G/t_G}$) of 8.0 mm/yr and single-standard-deviation uncertainty in slip rate ($\varepsilon_{\mathbf{d/t}}$) of ±0.7 mm/yr using the formula:

$$\varepsilon_{\mathbf{d/t}} = \{(\varepsilon_d/\mathbf{t})^2 + [(\mathbf{d}*\varepsilon_t)/\mathbf{t}^2]^2\}^{1/2}.$$

For apex E slip ($\mathbf{d_E}$) is ~42 m and the single-standard-deviation uncertainty in the slip (ε_d) is ~6 m based on the ε_{rms} of component slip errors ($\varepsilon_{\mathbf{SW}} \sim 2$ m; $\varepsilon_{\mathbf{NE}} \sim 5.5$ m). The age of inception of flow from apex E ($\mathbf{t_E}$) is 4580 years (before 1990) and single-standard-deviation uncertainty in the age (ε_t) is 50 years. The slip rate based on apex E ($\mathbf{d_E/t_E}$) is thus 9.2 mm/yr with single-standard-deviation uncertainty in slip rate ($\varepsilon_{\mathbf{d/t}}$) of ±1.3 mm/yr.

Conclusions

The minimum post-8.27 ka slip rate of 8.0 ± 0.7 mm/yr at this site clearly demonstrates that the Hayward fault moves significantly faster over millenia than the present surface creep rate, 4.7 ± 0.1 mm/yr over the past 14 years at Appian Way (<0.6 km southeast of the site). Thus deeper parts of the fault must be currently locked and accumulating shear strain for large earthquakes [*Lienkaemper et al.*, 1991; *Savage and Lisowski*, 1993]. The other rate at this site for the middle Holocene (9.2 ± 1.3 mm/yr since 4.58 ka) corroborates that geologic rate exceed creep rates but is not sufficiently accurate to prove that any significant difference in long-term rate has occurred over the last 8.27 kyr.

We emphasize that the 8.0 mm/yr should be regarded as a firm minimum because we believe that our geologic slip indicator, the stream channels, do not span the probable total width of the active fault deformation zone at the site. Thus a more inclusive estimate of long-term slip rate on the Hayward fault may be the highest creep rates of ~9 mm/yr documented in southern Fremont [*Lienkaemper et al.*, 1991]. Even 9 mm/yr may represent a minimum long-term slip rate, because this fast creeping segment of the fault distinctly ruptured to the surface in 1868, indicating a locked patch at depth.

Acknowledgments. We are deeply grateful to the Masonic Home directors, management, and staff for their considerable interest, cooperation, and valued assistance. Gladaway Gardens kindly squeezed us into their busy flower growing seasons. Principal funding was from the National Earthquake Hazards Reduction Program of the U.S. Geological Survey; much additional funding came from the California Division of Mines and Geology. J. C. Hamilton developed the total station map of the site. J. F. Wilmesher, D. Meier, and T. J. Powers ably assisted in logging the trenches. J. D. Sims and M. M. Clark reviewed the 1990 trench and contributed timely insights into some difficult stratigraphic issues. Thanks also to reviewers S. Hecker, D. J. Ponti, P. W. Williams, K. I. Kelson, and R. S. Yeats, whose comments made this a more rigorous and a clearer paper.

References

Biasi, G. P., and R. Weldon, Quantitative refinement of calibrated ^{14}C distributions, *Quat. Res.*, *41*, 1–18, 1994.

Borchardt, G., J. J. Lienkaemper, and K. E. Budding, Holocene slip rate of the Hayward fault in Fremont, California, in *Proceedings of the Second Conference on Earthquake Hazards in the Eastern San Francisco Bay Area, March 25–29, 1992, California State University, Hayward*, edited by G. Borchardt et al., *Spec. Publ. Calif. Div. Mines Geol.*, *113*, 181–188, 1992.

Brocher, T. M., et al., Seismic evidence for a lower-crustal detachment beneath San Francisco Bay, California, *Science*, *265*, 1346–1349, 1994.

Dibblee, T. W., Jr., Preliminary geologic maps of the La Costa Valley, Livermore, and Niles quadrangles, Alameda and Contra Costa Counties, California, scale 1:24,000, *U.S. Geol. Surv. Open File Rep.*, *80-533*, 3 sheets, 1980.

Galehouse, J. S., Theodolite measurements of creep rates on San Francisco Bay region faults, in *National Earthquake Hazards Reduction Program, Summaries of Technical Reports*, vol. XXXV, compiled

by M. Jacobson, *U.S. Geol. Surv. Open File Rep., 94-176*, 328–338, 1994.

Lawson, A. C., The Earthquake of 1868, in The California earthquake of April 18, 1906, in *Report of the State Earthquake Investigation Commission*, vol. I, pp. 434–438, Carnegie Inst. of Washington, Washington, D. C., 1908. (Reprinted 1969.)

Lienkaemper, J. J., Slip history of San Andreas and Hayward faults, in *National Earthquake Hazards Reduction Program, Summaries of Technical Reports*, vol. XXIX, compiled by M. Jacobsen, *U.S. Geol. Surv. Open File Rep., 90-54*, 89–91, 1990.

Lienkaemper, J. J., Map of recently active traces of the Hayward fault, Alameda and Contra Costa counties, California, scale 1:24,000, *U.S. Geol. Surv. Misc. Field Stud. Map, MF-2196*, 13 pp., 1992a.

Lienkaemper, J. J., Optional stop A-4, Masonic Home slip rates, in *Field Trip Guidebook of the Second Conference on Earthquake Hazards in the Eastern San Francisco Bay Area, March 25–29, 1992*, edited by N. T. Hall and M. Melody, p. 173, Calif. State Univ., Hayward, 1992b.

Lienkaemper, J. J., and J. C. Hamilton, Stop A-3, Holy Sepulchre fault scarp, in *Field Trip Guidebook of the Second Conference on Earthquake Hazards in the Eastern San Francisco Bay Area, March 25–29, 1992*, edited by N. T. Hall and M. Melody, pp. 151–156, Calif. State Univ., Hayward, 1992.

Lienkaemper, J. J., G. Borchardt, and M. Lisowski, Historic creep rate and potential for seismic slip along the Hayward fault, California, *J. Geophys. Res., 96*, 18,261–18,283, 1991.

Linick, T. W., A. Long, P. E. Damon, and C. W. Ferguson, High-precision radiocarbon dating of bristlecone pine from 6554 to 5350 B.C., *Radiocarbon, 28*, 943–953, 1986.

Lisowski, M., J. C. Savage, and W. H. Prescott, The velocity field along the San Andreas fault, *J. Geophys. Res., 96*, 8369–8390, 1991.

Perkins, J. B., Assessing the vulnerability of the built environment of the East Bay to earthquake hazards, in *Proceedings of the Second Conference on Earthquake Hazards in the Eastern San Francisco Bay Area, March 25–29, 1992, California State University, Hayward, Spec. Publ. Calif. Div. Mines Geol., 113*, 443–449, 1992.

Savage, J. C., and M. Lisowski, Inferred depth of creep on the Hayward fault, central California, *J. Geophys. Res., 98*, 787–793, 1993.

Steinbrugge, K. V., J. H. Bennett, H. J. Lagorio, J. F. Davis, G. Borchardt, and T. R. Toppozada, Earthquake planning scenario for a magnitude 7.5 earthquake on the Hayward fault in the San Francisco Bay area, *Spec. Publ. Calif. Div. Mines Geol., 78*, 243 pp., 1987.

Stuiver, M., and P. J. Reimer, Extended ^{14}C database and revised CALIB radiocarbon calibration program, *Radiocarbon, 35*, 215–230, 1993.

Stuiver, M., T. F. Braziunas, B. Becker, and B. Kromer, Climatic, solar, oceanic and geomagnetic influences of Late-Glacial and Holocene atmospheric $^{14}C/^{12}C$ change, *Quat. Res., 35*, 1–24, 1991.

Wallace, R. E. (Ed.), The San Andreas fault system, California, *U.S. Geol. Surv. Prof. Pap., 1515*, 283 pp., 1990.

Working Group on California Earthquake Probabilities, Probabilities of large earthquakes occurring in the San Francisco Bay Region, California, *U.S. Geol. Surv. Circ., 1053*, 51 pp., 1990.

G. Borchardt, Soil Tectonics, P.O. Box 5335, Berkeley, CA 94705.
J. J. Lienkaemper, U.S. Geological Survey, 345 Middlefield Road, MS 977, Menlo Park, CA 94025. (e-mail: jlienk@isdmnl.wr.usgs.gov)

(Received September 28, 1994; revised April 28, 1995;
accepted May 2, 1995.)